Original article

Discovery of 4-(dihydropyridinon-3-yl)amino-5-methylthieno[2,3-*d*]pyrimidine derivatives as potent Mnk inhibitors: synthesis, structure–activity relationship analysis and biological evaluation

Mingfeng Yu, Peng Li, Sunita K.C. Basnet, Malika Kumarasiri, Sarah Diab, Theodosia Teo, Hugo Albrecht, Shudong Wang*

Centre for Drug Discovery and Development, Sansom Institute for Health Research and Center for Cancer Biology, School of Pharmacy and Medical Sciences, University of South Australia, Adelaide, South Australia 5001, Australia

A B S T R A C T

Phosphorylation of the eukaryotic initiation factor 4E (eIF4E) by mitogen-activated protein kinase (MAPK)-interacting kinases (Mnks) is essential for oncogenesis but unnecessary for normal development. Thus, pharmacological inhibition of Mnks may offer an effective and non-toxic anti-cancer therapeutic strategy. Herein, we report the discovery of 4-(dihydropyridinon-3-yl)amino-5-methylthieno [2,3-*d*]pyrimidine derivatives as potent Mnk inhibitors. Docking study of **7a** in Mnk2 suggests that the compound is stabilised in the ATP binding site through multiple hydrogen bonds and hydrophobic interaction. Cellular mechanistic studies on MV-4-11 cells with leads **7a**, **8e** and **8f** reveal that they are able to down-regulate the phosphorylated eIF4E, Mcl-1 and cyclin D1, and induce apoptosis.

© 2015 Elsevier Masson SAS. All rights reserved.

1. Introduction

Dysregulation of protein synthesis is implicated in the progression of various pathologies, most notably cancer [1]. As a key rate-limiting step in protein synthesis, initiation of cap-dependent translation is contingent on the availability and activity of the eukaryotic initiation factor 4E (eIF4E) [2]. This general translation factor is regulated by mitogen-activated protein kinase (MAPK)-interacting kinases (Mnks) through phosphorylation at Ser209 [3]. The phosphorylation process is necessary for oncogenic transformation [4,5]. Perturbation of the process by mutating eIF4E at Ser209 [6], silencing Mnk1 with small hairpin RNA (shRNA) [7] or knocking out Mnk1/2 [7] attenuated or even prevented tumour formation. Conversely, activation of Mnk1 promoted tumourigenesis in a manner similar to eIF4E [8]. In contrast with their pivotal role in tumourigenesis, Mnks seem to be dispensable for normal development [4,5]. For example, neither cap-dependent translation nor global protein synthesis was influenced in Mnk-deficient embryonic fibroblasts [9]. Taken together, these

biological studies provide a rationale for the potential application of specific Mnk inhibition as an effective and non-toxic therapeutic strategy against cancer. Hence, there is a pressing demand in discovering pharmacologically selective Mnk inhibitors.

Regrettably, little progress has been made in the discovery of pharmacological Mnk inhibitors since the first isolation and identification of the two kinases in 1997 [3,10]. The known Mnk inhibitors include CGP052088 [11], CGP57380 [12,13], cercosporamide [14] and hypothemycin derivatives [15–17] (Fig. 1). These small molecules inhibit Mnks at nanomolar to micromolar concentrations. However, all of them target multiple protein kinases. Earlier this year, a series of 5-(2-(phenylamino)pyrimidin-4-yl)thiazol-2(3*H*)-one derivatives was reported as potent Mnk2 inhibitors with sub-micromolar affinity, but the kinase selectivity remains unconquered [18].

The high structural similarity of the ATP binding pockets among kinases renders selective Mnk inhibition by exogenous inhibitors challenging. Previous crystallographic analyses of Mnks reveal two distinct structural features: (i) a noncanonical DFD motif (*vs.* a common DFG motif in other kinases) and (ii) three Mnk-specific inserts (*i.e.*, insertions I1, I2 and I3) at the catalytic domain [19,20]. In the absence of a ligand, Mnks predominantly adopt an
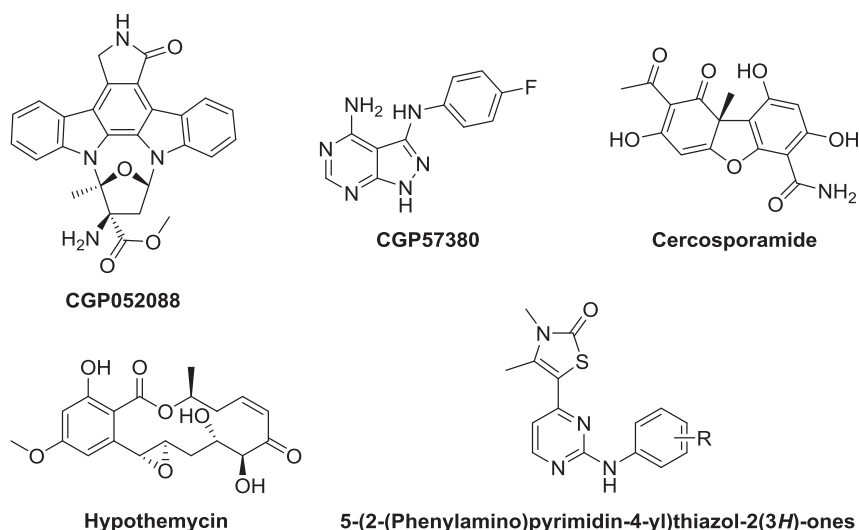
Fig. 1. Chemical structures of known Mnk inhibitors.

unusual DFD-out conformation, in which the Phe residue flips into the ATP binding pocket, thus preventing the accessibility of ATP [21]. Exploiting the above characteristics would assist in the rational design of highly selective Mnk inhibitors. Nevertheless, the lack of structural details on the ATP-bound Mnks has hampered the development of specific Mnk inhibitors.

In our earlier attempt to identify novel selective Mnk inhibitors, the ChemBridge database consisting of approximately 572,000 molecules was pre-filtered according to molecular weights, and the remaining 387,000 compounds with molecular weights ranging from 300 to 450 were subjected to a comprehensive virtual screening using both protein- and ligand-based approaches. In the former method, the only available staurosporine-bound Mnk2 (D228G) crystal structure (PDB ID: 2HW7) was adopted to create a binding site for the protein-ligand docking. In the latter approach, CGP57380 and cercosporamide, two most extensively studied Mnk inhibitors, were selected as query molecules for the ligand-based alignment. Successful deployment of these two methods was followed by structure-guided optimisation and the evaluation of Mnk inhibitory activity of the remaining candidates using biochemical assays to reveal 4-aminothieno[2,3-d]pyrimidine as a valuable chemical scaffold for Mnk inhibitors [22]. Using analogue-based drug design, we further explored the utility and versatility of this scaffold. Herein, we describe the synthesis and biological evaluation of 4-(dihydropyridinon-3-yl)amino-5-methylthieno[2,3-d]pyrimidine derivatives.
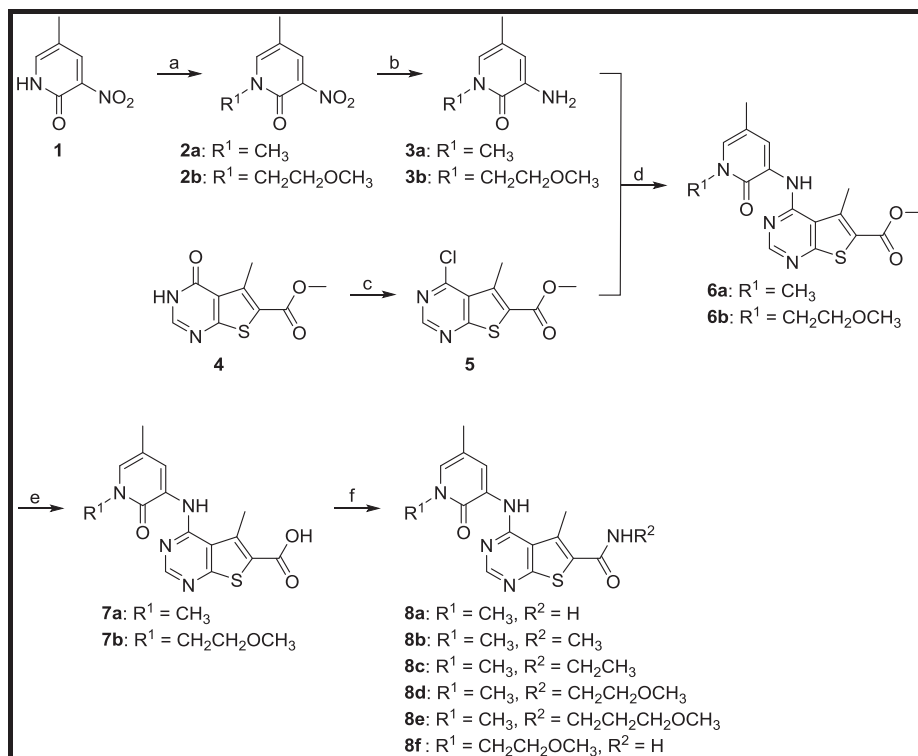
2. Results and discussion

2.1. Chemistry

The synthetic route deployed to prepare methyl 4-((1-alkyl-2-oxo-5-methyl-1,2-dihydropyridin-3-yl)amino)-5-methylthieno[2,3-d]pyrimidine-6-carboxylates (6a and 6b) and their derivatives (7a, 7b and 8a−f) is delineated in Scheme 1. N-Alkylation of 5-methyl-3-nitropyridin-2(1H)-one 1 with iodomethane or 1-bromo-2-methoxyethane in the presence of potassium carbonate gave 1,5-dimethyl-3-nitropyridin-2(1H)-one 2a or 1-(2-methoxyethyl)-5-methyl-3-nitropyridin-2(1H)-one 2b respectively in good yields (2a: 95% and 2b: 60%), which underwent palladium-catalysed hydrogenation to afford the corresponding 3-amino-1,5-dimethylpyridin-2(1H)-one 3a or 3-amino-1-(2-

methoxyethyl)-5-methylpyridin-2(1H)-one 3b in excellent yields (3a: 94% and 3b: 100%). Chlorination of methyl 5-methyl-4-oxo-3,4-dihydrothieno[2,3-d]pyrimidine-6-carboxylate 4 with thionyl chloride in the presence of N,N-dimethylformamide (DMF) yielded methyl 4-chloro-5-methylthieno[2,3-d]pyrimidine-6-carboxylate 5 in a yield of 89%. Each of amines 3a and 3b was individually coupled with chloride 5 in the presence of p-toluenesulfonic acid under microwave irradiation to give the corresponding methyl 4-((1-alkyl-2-oxo-5-methyl-1,2-dihydropyridin-3-yl)amino)-5-methylthieno[2,3-d]pyrimidine-6-carboxylates 6a and 6b in good yields (6a: 86% and 6b: 54%), which were subsequently subjected to saponification in an alkaline methanolic solution to yield the carboxylic acids 7a and 7b respectively in excellent yields (7a: 100% and 7b: 84%). Amination of carboxylic acids 7a and 7b with appropriate amines was effected in anhydrous DMF in the presence of the coupling reagent 1-[bis(dimethylamino)methylene]-1H-1,2,3-triazolo[4,5-b]pyridinium 3-oxid hexafluorophosphate (HATU) and N,N-diisopropylethylamine (DIPEA) to give the corresponding amides 8a-f in moderate to good yields (36—80%).
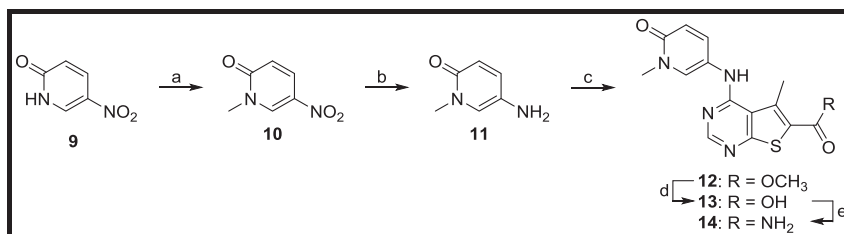
The above synthetic approach was successfully applied to the preparation of methyl 4-((1-methyl-6-oxo-1,6-dihydropyridin-3-yl)amino)-5-methylthieno[2,3-d]pyrimidine-6-carboxylate (12) and its derivatives (13 and 14) (Scheme 2). In brief, 5-nitropyridin-2(1H)-one 9 sequentially underwent alkylation and reduction to give 5-amino-1-methylpyridin-2(1H)-one 11. Due to its instability in the air, amine 11 was directly used in the next synthetic step without further purification and characterisation; p-toluenesulfonic acid-catalysed substitution of chloride 5 with amine 11 was achieved by microwave irradiation to give the desired methyl 4-((1-methyl-6-oxo-1,6-dihydropyridin-3-yl)amino)-5-methylthieno[2,3-d]pyrimidine-6-carboxylate 12. Ester 12 was readily hydrolysed to afford carboxylic acid 13 in a yield of 88%, which was subsequently aminated with ammonia to give amide 14 in 54% yield.

2.2. Structure−activity relationship analysis

Up-regulation of eIF4E is observed in acute myeloid leukaemia (AML) [23] and targeting eIF4E by pharmacologic inhibition of its activating kinases Mnks may provide a new approach for the treatment of AML. A recent study demonstrated that the suppressive effects of cercosporamide on AML correlated with its Mnk

Scheme 1. Synthesis of methyl 4-((1-alkyl-2-oxo-5-methyl-1,2-dihydropyridin-3-yl)amino)-5-methylthieno[2,3-d]pyrimidine-6-carboxylates (**6a–b**) and their derivatives (**7a–b** and **8a–f**). *Reagents and conditions*: (a) appropriate alkyl halide, K₂CO₃, DMF, 0 °C to rt for CH₃I, 0 °C to 70 °C for BrCH₂CH₂OCH₃, o/n, **2a**: 95%, **2b**: 60%; (b) H₂, 10% Pd/C, CH₃OH, rt, o/n, **3a**: 94%, **3b**: 100%; (c) SOCl₂, DMF, reflux, 2 h, 89%; (d) TsOH·H₂O, 1,4-dioxane, microwave 200—300 W, 150 °C, 30 min, **6a**: 86%, **6b**: 54%; (e) 2 M NaOH, CH₃OH, reflux, 2 h, **7a**: 100%, **7b**: 84%; (f) appropriate amine, HATU, DIPEA, DMF, 0 °C to rt, o/n, **8a**: 80%, **8b**: 36%; **8c**: 66%; **8d**: 58%; **8e**: 37%; **8f**: 66%.

Scheme 2. Synthesis of methyl 4-((1-methyl-6-oxo-1,6-dihydropyridin-3-yl)amino)-5-methylthieno[2,3-d]pyrimidine-6-carboxylate (**12**) and its derivatives (**13** and **14**). *Reagents and conditions*: (a) CH₃I, K₂CO₃, DMF, 0 °C to rt, o/n, 99%; (b) H₂, 10% Pd/C, CH₃OH, rt, o/n; (c) **5**, TsOH·H₂O, 1,4-dioxane, microwave 200—300 W, 150 °C, 30 min, 68% over steps (b) and (c); (d) 2 M NaOH, CH₃OH, rt, 48 h, 88%; (e) NH₃ (0.5 M in 1,4-dioxane), HATU, DIPEA, DMF, 0 °C to rt, o/n, 54%.
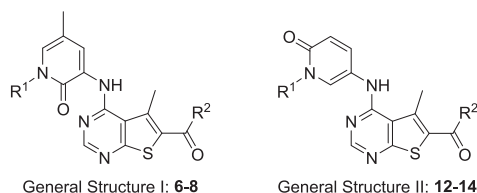
inhibitory activity [24], supporting the potential application of pharmacologic Mnk inhibitors in anti-leukaemia therapy. As one of the most studied AML cell lines, MV-4-11 was selected for cell viability assay and cellular mechanistic investigation (*vide infra*) due to its increasing use for the assessment of anti-leukaemic effects of Mnk inhibition [18,24,25] as well as its sensitivity to Mnk inhibitors [18,22].

Mnk inhibitory activity of compounds **6–8** and **12–14** was evaluated using the ADP-Glo™ kinase assay [26], and the anti-proliferative activity tested by a cell viability assay using resazurin [18]. CGP57380, a known Mnk inhibitor, served as a positive control for both enzymatic and cellular assays. The results obtained from these biological assays are summarised in Table 1. All methyl esters (R^2 = OCH₃), *i.e.*, **6a** (R^1 = CH₃ in general structure I), **6b** (R^1 = CH₂CH₂OCH₃) and **12** (R^1 = CH₃ in general structure II), are not active against both Mnk1 and Mnk2 with K_i values being greater than 10 μM, and are moderately toxic against MV-4-11 cells with GI₅₀ values ranging from 13.44 to 47.82 μM. Both kinase

inhibitory activity and cytotoxicity are consistent with the results previously obtained for methyl 4-(phenylamino)-5-methylthieno[2,3-d]pyrimidine-6-carboxylates [22]. Conversion of the methyl ester moiety into the carboxylic acid group resulting in **7a** (R^1 = CH₃, R^2 = OH in general structure I), **7b** (R^1 = CH₂CH₂OCH₃, R^2 = OH) and **13** (R^1 = CH₃, R^2 = OH in general structure II), dramatically boosts the inhibitory activity against both Mnks, implying the involvement of the carboxylic acid in the interaction with the kinases. Carboxylic acids **7a**, **7b** and **13** inhibit Mnk1 and Mnk2 with K_i values in the range of 2.06–4.82 μM and 0.24–0.90 μM respectively, which are comparable and superior to those of CGP57380 (K_i = 1.01 μM for Mnk1 *vs.* K_i = 0.88 μM for Mnk2). Compound **7a** possesses the highest selectivity towards Mnk2 over Mnk1 by approximate 14-fold (K_i = 4.82 μM for Mnk1 *vs.* K_i = 0.35 μM for Mnk2), whereas compound **7b** represents the most potent dual Mnk inhibitor with K_i values of 2.06 μM for Mnk1 and 0.24 μM for Mnk2. Despite the significant improvement in Mnk inhibitory activity, carboxylic acids **7a**, **7b** and **13** display lower or at

Table 1
Summary of chemical structures and their biological activities.

General Structure I: **6-8**   General Structure II: **12-14**

| Compound	R^1	R^2	Mnk inhibition K_i (μM)[a]		Anti-proliferation GI_{50} (μM)[b]
			Mnk1	Mnk2	MV-4-11
6a	CH_3	OCH_3	>10	>10	13.44 ± 0.70
6b	$CH_2CH_2OCH_3$	OCH_3	>10	>10	26.22 ± 2.70
7a	CH_3	OH	4.82	0.35	15.18 ± 1.91
7b	$CH_2CH_2OCH_3$	OH	2.06	0.24	59.58 ± 3.48
8a	CH_3	NH_2	>10	>10	17.51 ± 1.02
8b	CH_3	$NHCH_3$	>10	9.05	10.37 ± 2.80
8c	CH_3	$NHCH_2CH_3$	>10	5.99	9.66 ± 0.72
8d	CH_3	$NHCH_2CH_2OCH_3$	5.40	3.17	11.30 ± 3.81
8e	CH_3	$NHCH_2CH_2CH_2OCH_3$	5.00	2.63	5.73 ± 0.38
8f	$CH_2CH_2OCH_3$	NH_2	2.33	0.34	13.96 ± 2.21
12	CH_3	OCH_3	>10	>10	47.82 ± 13.84
13	CH_3	OH	2.15	0.90	88.99 ± 4.11
14	CH_3	NH_2	4.51	1.60	89.59 ± 13.62
CGP57380	–	–	1.01	0.88	4.88 ± 0.45

[a] K_m values were used as ATP concentrations. Apparent inhibition constants (K_i) were calculated using IC_{50} values and appropriate K_m (ATP) values for each kinase, and are expressed as mean values derived from two replicates.
[b] GI_{50} values were determined by 72 h resazurin assay, and are presented as mean ± standard deviation derived from at least two replicates.

the best similar cytotoxicity in comparison with the corresponding methyl esters **6a**, **6b** and **12** (GI_{50} > 15 μM for carboxylic acids *vs.* GI_{50} > 13 μM for methyl esters). Amination of carboxylic acids reduces or even abolishes Mnk inhibitory activity. Accordingly, carboxamides **8f** (R^1 = $CH_2CH_2OCH_3$, R^2 = NH_2) and **14** (R^1 = CH_3, R^2 = NH_2 in general structure II) show marginally weaker Mnk inhibitory potency than do the corresponding carboxylic acids **7b** and **13**, whereas carboxamide **8a** (R^1 = CH_3, R^2 = NH_2 in general structure I) loses inhibitory activity against both Mnks (K_i > 10 μM). The distinct kinase inhibitory activities between **8a** and each of **8f** and **14** imply that both the nature of R^1 substituent and the topology of the dihydropyridinone ring are important factors for the affinity for Mnks. The anti-proliferative effects of **8a** and **14** (with their respective GI_{50} values of 17.51 and 89.59 μM) on MV-4-11 cells are comparable to those of the corresponding carboxylic acids **7a** and **13**, whereas **8f** shows a significantly enhanced anti-proliferative activity by comparison to its carboxylic acid counterpart **7b** (GI_{50} = 59.58 μM for **7b** *vs.* GI_{50} = 13.96 μM for **8f**). *N*-Alkylation of the carboxamide **8a** restores Mnk inhibitory activity and enhances cytotoxicity. Along with the increase in the alkyl chain length, Mnk inhibitory activity improves with the selectivity towards Mnk2. However, Mnk inhibitory activities of all carboxamides, *i.e.*, **8a-e**, decrease when compared to the parent carboxylic acid **7a**, suggesting a preferable role of the carboxylic acid in the interaction with Mnks. All *N*-monoalkylated carboxamides, *i.e.*, **8b-f**, demonstrate potent anti-proliferative activity with GI_{50} values ranging from 5.73 to 11.30 μM. Compound **8e** with the longest chain (R^1 = CH_3, R^2 = $NHCH_2CH_2CH_2OCH_3$) exhibits the highest toxicity against MV-4-11 cells with a GI_{50} value of 5.73 μM, which is comparable with that of CGP57380 (GI_{50} = 4.88 μM).

Taken together, low micromolar to sub-micromolar Mnk inhibition has been achieved with the 4-(dihydropyridinon-3-yl)amino-thieno[2,3-*d*]pyrimidine framework. The selectivity of Mnk2 over Mnk1 can be optimised by (i) manipulating the topology and/or *N*-substitution of the dihydropyridinone ring, and/or (ii) varying the C-6 functionality at the thieno[2,3-*d*]pyrimidine moiety.

However, it appears to be a discrepancy between Mnk inhibitory potency and cellular anti-proliferative effects, and two plausible explanations are: (i) *in vitro* inhibition of Mnks at low micromolar or sub-micromolar concentrations may not necessarily cause cell death during the 72-h incubation, and/or (ii) the tested compounds may also target other kinase(s), both of which from a biochemical standpoint warrant the further investigation of these Mnk inhibitors in kinase and cell panel screens. Thus, **7a**, **7b** and **8e** were tested against a panel of 9 kinases, including cyclin-dependent kinases (*i.e.*, CDK2/cyclinA and CDK9/cyclinT1), Mnk upstream activating kinases in Ras/Raf/MAPK and PI3K/Akt/mTOR pathways (*i.e.*, MAPK1, mTOR, PKBα, SAPK2a and PI3K), as well as FLT3 and Pim-1. The results obtained from this kinase panel screen are presented in Fig. 2. Both **7a** and **7b** have no inhibitory activity against all kinases tested at the concentration of 10 μM, confirming their selectivity for Mnks and their potential use as pharmacologic tools for the
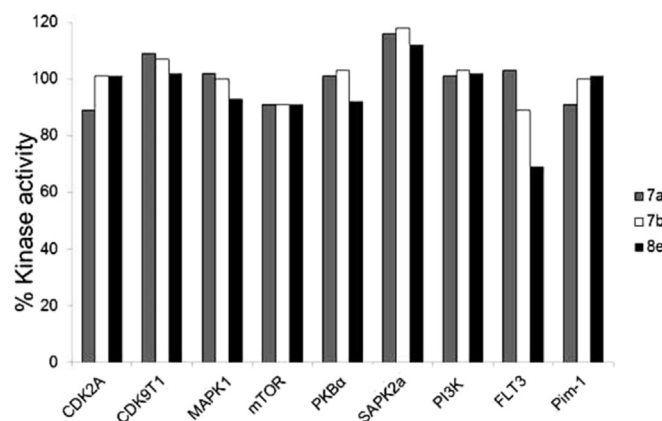
Fig. 2. Selectivity of kinase inhibition by compound **7a**, **7b** and **8e**. Compounds were tested at the concentration of 10 μM. ATP concentrations used were within 15 μM of K_m values.
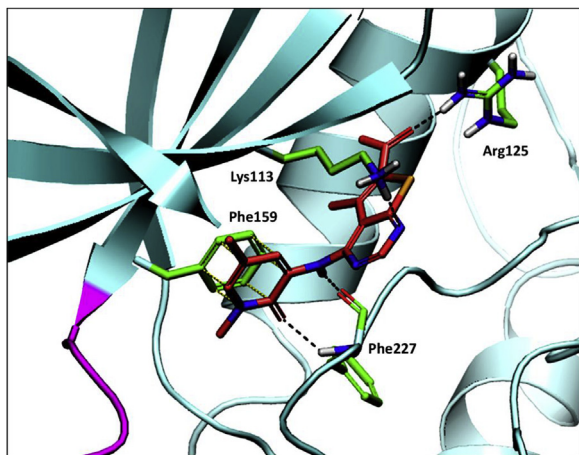
Fig. 3. Proposed binding mode of **7a** to the ATP-binding pocket of Mnk2. **7a** is engaged in four hydrogen bonds and a π-π stacking interaction with the protein. The protein is depicted as cyan ribbons with the hinge region in magenta. Nitrogen atoms are shown in blue, sulphur atom in yellow, oxygen atoms in red, hydrogen atoms in grey, receptor carbon atoms in green, and ligand carbon atoms in salmon. The glycine rich loop was omitted for clarity. The binding pose was generated by induced fit docking of **7a** to a DFD-in conformation model of Mnk2 using Schrödinger (Glide version 6.1, Prime version 3.4, Schrödinger, LLC, New York, NY, 2013). The figure was prepared using Pymol version 1.5.

evaluation of Mnk inhibition. Compound **8e** is not active against these kinases with the single exception of FLT3 where 31% inhibitory activity was detected. Given that FLT3 was previously suggested to be important for the proliferation and survival of AML cells [27] and that MV-4-11 cells express FLT3 protein [28], dual inhibitory activity of **8e** against both Mnks and FLT3 may contribute to its potent anti-proliferative effect.

2.3. Molecular basis for Mnk2 inhibitory activity

In order to understand the origins of the Mnk inhibitory potency of 4-(dihydropyridinon-3-yl)amino-5-methylthieno[2,3-*d*]pyrimidine derivatives, **7a** was docked to an in-house model of Mnk2 with the DFD-in conformation [29] using the induced fit protocol [30,31]. The docking was performed at the ATP binding pocket and the best scoring model was selected following visual inspection of the top scoring binding poses. Fig. 3 illustrates this plausible binding mode. **7a** is stabilised in the ATP binding pocket by four hydrogen bonds: the compound interacts with Phe227 of the DFD motif through the carbonyl oxygen atom of the dihydropyridinone ring and the NH linker, whereas the N-1 of the pyrimidine moiety and the carboxyl oxygen atom form two additional hydrogen bonds with positive-charged side chains of Lys113 and Arg125 respectively. Furthermore, the dihydropyridinone ring exhibits a π-π stacking interaction with the gatekeeper Phe159. Interestingly, no hinge region interactions, which are common among most kinase inhibitors, are observed. It appears that the salt bridge between the carboxylate moiety of **7a** and the guanidine side chain of Arg125 makes a significant contribution to the binding affinity. When the carboxylate moiety is replaced by a methyl ester group (**6a**), the interaction with Arg125 is severed, reducing the binding affinity. On the other hand, removal of the negative charge from the carboxylate moiety by the substitution with an amide group appears to disturb the binding mode in a subtle way. This substitution adversely affects the binding affinity in the case of **8a** while further replacement of the *N*-methyl group with an *N*-methoxyethyl chain (**8f**) may assist in recovering the binding affinity. To elucidate such subtle interplays between substituents, more rigorous calculations, potentially assisted by experimental structure determinations, are

required.

2.4. Cellular mechanism of action

Carboxylic acid **7a** is the most selective Mnk2 inhibitor whereas *N*-(3-methoxypropyl) carboxamide **8e** displays the highest cytotoxicity against MV-4-11 cells. Thus, these two molecules were chosen for detailed cellular mechanistic investigation. Carboxamide **8f** was also selected in virtue of its well-balanced biological activity, *i.e.*, high potency in both Mnk inhibition and antiproliferation. CGP57380 was employed as a positive control. Compounds were tested at concentrations which are approximately twice as much as their respective GI$_{50}$ values (2 × GI$_{50}$) with the exception of **8e** which was used at the concentration of approximately 4 × GI$_{50}$ value, *i.e.*, **7a** and **8f** at 30 μM, **8e** at 20 μM and CGP57380 at 10 μM.

Cell death occurs through several pathways including apoptosis, autophagocytosis and necrosis. To evaluate whether apoptosis contributes to the anti-proliferative effects of **7a**, **8e** and **8f**, annexin V/propidium iodide (PI) staining of MV-4-11 cells was carried out upon incubation with each compound for 24 h (Fig. 4A). In comparison with DMSO diluent, **7a**, **8e** and **8f** induced more apoptotic cells (annexin V+/PI- and annexin V+/PI+) by 6–10%. CGP57380 was more effective in inducing apoptosis, resulting in an increment of 13% apoptotic cells.

To determine whether the apoptosis observed with **7a**, **8e** or **8f** is caspase-dependent, MV-4-11 cells were treated with each compound for 24 h, and the activity of caspases 3 and 7 was measured (Fig. 4B). No significant changes in caspase 3/7 activity were observed, which is in agreement with the previous results obtained with 5-(2-(phenylamino)pyrimidin-4-yl)thiazol-2(3*H*)-one derivatives [18].

To further assess whether the anti-proliferative effect of **7a**, **8e** or **8f** is a consequence of inhibition of cell cycle progression, MV-4-11 cells were exposed to each compound for 24 h, and analysed by flow cytometry. A similar cell cycle profile was observed for the cells treated with **7a**, **8e** or **8f** (Fig. 4C). Each compound caused a marked increase in the population of G1-phase cells and a minor accumulation of sub-G1-phase cells, which was companied by a substantial loss in S- and G2/M-phase cells. These results are consistent with previously reported observations on alternative Mnk inhibitors [18,22].

To investigate cellular Mnk inhibitory potency of **7a**, **8e** or **8f**, MV-4-11 cells were incubated with each compound for 24 h, and analysed by Western blot (Fig. 4D). Treatment with **7a**, **8e** or **8f** abolished the phosphorylation of eIF4E at Ser209, but barely affected the levels of Mnk1 and total eIF4E, confirming their cellular Mnk inhibitory activity. CGP57380 also reduced the level of phosphorylated eIF4E. **7a**, **8e** and **8f** were capable of down-regulating anti-apoptotic protein myeloid cell leukaemia 1 (Mcl-1) and causing poly (ADP-ribose) polymerase (PARP) cleavage, both of which are associated with the apoptosis observed in MV-4-11. CGP57380 exerted similar effects on Mcl-1 and PARP. **7a**, **8e** and **8f** moderately to significantly blocked the expression of cyclin D1, which well correlates with the observation that these molecules induced G1 cell cycle arrest (*vide supra*).

3. Conclusions

A series of 4-(dihydropyridinon-3-yl)amino-5-methylthieno [2,3-*d*]pyrimidine derivatives was synthesised and their structure activity relationships were investigated. Many compounds displayed potent Mnk inhibitory activity with the selectivity towards Mnk2. The induced fit docking study with a DFD-in conformation model of Mnk2 implies **7a** is stabilised in the ATP binding pocket by
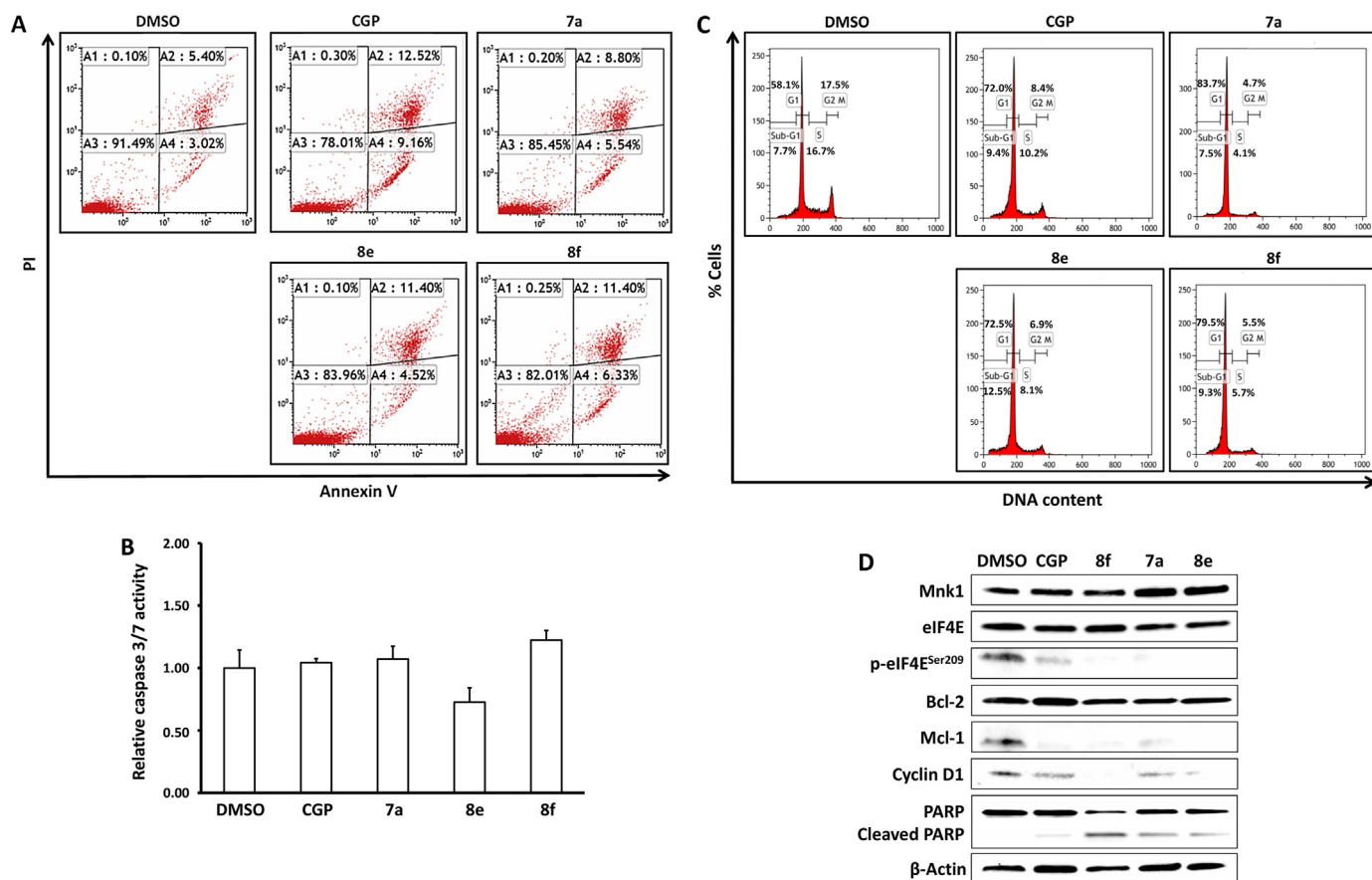
Fig. 4. Cellular mechanism of action of **7a**, **8e** and **8f**. (A) Induction of apoptosis by **7a**, **8e**, **8f** or CGP57380 in MV-4-11 cells. Cells were exposed to each compound for 24 h, and analysed by Annexin V/PI staining. The percentage of cells undergoing apoptosis is defined as the sum of early apoptotic (annexin V+/PI-) cell percentage and late apoptotic (annexin V+/PI+) cell percentage. (B) Relative caspase 3/7 activity in MV-4-11 cells after treatment with **7a**, **8e**, **8f** or CGP57380 for 24 h. (C) Cell cycle analysis of MV-4-11 cells after incubation with **7a**, **8e**, **8f** or CGP57380 for 24 h. (D) Western blot analysis of MV-4-11 cells treated with **7a**, **8e**, **8f** or CGP57380 for 24 h. β-Actin antibody was used as an internal control. In all experiments, DMSO diluent was employed as a control, and compounds were tested at concentrations of their respective ($2 \times GI_{50}$) values with the exception of **8e** which was used at the concentration of approximately $4 \times GI_{50}$ value, *i.e.*, **7a** and **8f** at 30 μM, **8e** at 20 μM and CGP57380 at 10 μM.

four hydrogen bonds and hydrophobic interaction. Cellular mechanistic studies on MV-4-11 cells with lead compounds **7a**, **8e** and **8f** reveal that they are able to block the phosphorylation of eIF4E *via* targeting Mnks, down-regulate Mcl-1 and cause PARP cleavage. This study suggests that exploration of the structural diversity in the context of 4-aminothieno[2,3-*d*]pyrimidine would offer potent and highly selective Mnk inhibitors.

4. Experimental

4.1. Chemistry

All reactions except microwave-assisted syntheses were carried out with continuous magnetic stirring in ordinary glassware; microwave-assisted syntheses were performed in a 10 mL Asynt DrySyn insert (Isleham, UK) using a CEM Discover SP and Explorer 48/72/96 microwave system (Matthews, NC, USA) controlled by Synergy software (Firmware version DSCA02.17). Heating of reactions was conducted with a DrySyn® single- or multi-position heating block (Isleham, UK); cooling of reactions was achieved using an ice or ice-salt bath. All reagents and solvents (including anhydrous solvents) were purchased from Sigma–Aldrich, Alfa Aesar, Merck, GL Biochem, Combi-block or Ajax Finechem, and were used as received. Methyl 5-methyl-4-oxo-3,4-dihydrothieno [2,3-*d*]pyrimidine-6-carboxylate (**4**) was purchased from Le Sun Pharmaceuticals (China). ^{1}H and ^{13}C NMR spectra were recorded at

298 K on a Bruker AVANCE III HD 500 spectrometer (^{1}H at 500.16 MHz and ^{13}C at 125.76 MHz; Faellanden, Switzerland), and were analysed using Bruker Topspin 3.2 software. ^{1}H and ^{13}C NMR spectra are referenced to ^{1}H signals of residual nondeuterated solvents and ^{13}C signals of deuterated solvents respectively. ^{1}H NMR signals are reported with chemical shift values δ (ppm), multiplicity (s = singlet, d = doublet, t = triplet, q = quartet, dd = doublet of doublets, m = multiplet and br = broad), relative integral, coupling constants *J* (Hz) and assignments. High resolution mass spectra were recorded on an AB SCIEX TripleTOF 5600 mass spectrometer (Concord, ON, Canada), and ionisation of all samples was carried out using ESI. Melting points were determined using an open capillary on a Stuart SMP10 melting point apparatus and are uncorrected. The purity of compounds used for biological evaluation was determined by analytic RP-HPLC which was carried out on a Shimadzu Prominence UFLC system (UltraFast Liquid Chromatograph, Kyoto, Japan) equipped with a CBM-20A communications bus module, a DGU-20A5R degassing unit, an LC-20AD liquid chromatograph pump, an SIL-20AHT auto-sampler, an SPD-M20A photo diode array detector, a CTO-20A column oven and a Phenomenex Kinetex 5u C18 100A 250 mm × 4.60 mm column. Method A (gradient 5%–95% CH_3OH containing 0.1% formic acid (FA) over 7 min at a flow rate of 1 mL/min, followed by 95% CH_3OH containing 0.1% FA over 13 min) and method B (gradient 5%–95% CH_3CN containing 0.1% FA over 7 min at a flow rate of 1 mL/min, followed by 95% CH_3CN containing 0.1% FA over 13 min) were used

for analytic RP-HPLC. Data acquired from analytic RP-HPLC were processed using LabSolutions Analysis Data System. Analytical TLC was performed on Merck silica gel 60 F_{254} pre-coated aluminium plates (0.2 mm) and visualised under UV light (254 nm). Column chromatography was carried out using a fritted solid loader packed with GRACE Davison DAVISIL® silica gel 60 Å (40–63 μm) on a Biotage FlashMaster Personal⁺ flash chromatography system.

General synthetic procedure A: N-Alkylation of pyridin-2(1H)-ones

To a suspension of pyridin-2(1H)-one (1.0 equiv.) and K_2CO_3 (2.0 equiv.) in DMF (0.60 M in pyridin-2(1H)-one) at 0 °C was added alkyl halide (1.5–2.0 equiv.) dropwise. The reaction mixture was allowed to warm up to room temperature (in the case of iodomethane) or heated at 70 °C (in the case of 1-bromo-2-methoxyethane), stirred overnight, concentrated under reduced pressure. The residue was diluted with H_2O (200 mL) and extracted with DCM (6 × 100 mL). The organic extracts were combined and concentrated under reduced pressure, and the residue was purified by Biotage® FlashMaster Personal⁺ flash chromatography (silica gel, DCM ramping to DCM:CH_3OH = 98:2 unless otherwise stated) to give the desired N-alkylated pyridine-2(1H)-one.

General synthetic procedure B: reduction of nitro compounds to amines

To a suspension of a nitro compound (1.0 equiv.) in CH_3OH (50 mM in nitro compound) was added 10% Pd/C (0.01 equiv.). The reaction mixture was bubbled with H_2 for 1 h at room temperature and stirred under H_2 overnight. The solids were filtered off and washed with DCM (25 mL). The filtrate and DCM washing were combined and concentrated under reduced pressure to give the desired amine.

General synthetic procedure C: substitution of chloride with amines

To a suspension of chloride **5** (1.0 equiv.) and amine (1.0 equiv.) in 1,4-dioxane (0.40 M in amine) was added TsOH·H_2O (0.20 equiv.). The reaction mixture was heated at 150 °C under microwave irradiation for 30 min, cooled down, and concentrated under reduced pressure. The residue was purified by Biotage® FlashMaster Personal⁺ flash chromatography (silica gel, DCM ramping to DCM:CH_3OH = 95:5 unless otherwise stated) to give the desired secondary amine.

General synthetic procedure D: hydrolysis of esters

To a suspension of ester (1.0 equiv.) in CH_3OH (50 mM in ester) was added 2 M NaOH (7.5 equiv.). The reaction mixture was heated at reflux for 2 h, cooled down to room temperature, and washed with DCM (20 mL). The aqueous layer was acidified with 2 M HCl to pH 3. The precipitate was filtered, washed with H_2O (3 × 25 mL), and dried under reduced pressure to give the desired carboxylic acid.

General synthetic procedure E: amide bond formation

To a suspension of the carboxylic acid (1.0 equiv.) in anhydrous DMF (3 mL) at 0 °C were added DIPEA (3.0 equiv. with the single exception of 10 equiv. in the case of methylamine hydrochloride) and HATU (1.1 equiv.). The reaction mixture was stirred at 0 °C for 10 min, and amine (5.0 equiv.) was added. The reaction mixture was allowed to warm up to room temperature, stirred under N_2 overnight and filtered. The solids were washed with ice-cold DMF (3 mL) and H_2O (30 mL) to give the desired amide.

4.1.1. 1,5-Dimethyl-3-nitropyridin-2(1H)-one (2a)

5-Methyl-3-nitropyridin-2(1H)-one (**1**, 1.39 g, 9.02 mmol) and iodomethane (840 μL, 13.5 mmol) were reacted using general synthetic procedure A to give **2a** as a yellow solid (1.44 g, 95%). **R$_F$**

(DCM:CH_3OH = 98:2) 0.49. **m.p.** 185–186 °C. ¹H NMR (CDCl₃) δ 2.18 (s, 3H, pyridinone-CH_3), 3.64 (s, 3H, NCH_3), 7.53 (d, 1H, J 1.5, pyridinone-H), 8.18 (d, 1H, J 2.5, pyridinone-H). ¹³C NMR (CDCl₃) δ 16.9, 38.7, 112.8, 138.0, 140.6, 143.2, 154.3. **HRMS** (ESI-TOF) *m/z* 191.0404 [M+Na]⁺; calcd. for $C_7H_8N_2NaO_3^+$ 191.0427 [M+Na]⁺.

4.1.2. 1-(2-Methoxyethyl)-5-methyl-3-nitropyridin-2(1H)-one (2b)

5-Methyl-3-nitropyridin-2(1H)-one (**1**, 1.54 g, 9.99 mmol) and 1-bromo-2-methoxyethane (1.88 mL, 20.0 mmol) were reacted using general synthetic procedure A. The residue was purified by Biotage® FlashMaster Personal⁺ flash chromatography (silica gel, EtOAc) to give **2b** as a yellow solid (1.27 g, 60%). **R$_F$** (EtOAc) 0.52. **m.p.** 103–105 °C. ¹H NMR (CDCl₃) δ 2.00 (s, 3H, pyridinone-CH_3), 3.10 (s, 3H, OCH_3), 3.48 (t, 2H, J 5.0, CH_2CH_2), 4.04 (t, 2H, J 5.0, CH_2CH_2), 7.49 (d, 1H, J 1.5, pyridinone-H), 8.02 (d, 1H, J 2.5, pyridinone-H). ¹³C NMR (CDCl₃) δ 16.3, 50.0, 58.4, 68.9, 112.0, 137.0, 140.4, 144.3, 153.3. **HRMS** (ESI-TOF) *m/z* 213.0847 [M+H]⁺; calcd. for $C_9H_{13}N_2O_4^+$ 213.0870 [M+H]⁺.

4.1.3. 3-Amino-1,5-dimethylpyridin-2(1H)-one (3a)

Nitro compound **2a** (169 mg, 1.00 mmol) was reduced according to general synthetic procedure B. The residue was purified by Biotage® FlashMaster Personal⁺ flash chromatography (silica gel, DCM ramping to DCM:CH_3OH = 98:2) to give **3a** as an orange oil (131 mg, 94%). **R$_F$** (DCM:CH_3OH = 98:2) 0.15. ¹H NMR (CDCl₃) δ 1.90 (s, 3H, pyridinone-CH_3), 3.42 (s, 3H, NCH_3), 4.15 (br s, 2H, NH_2), 6.33 (d, 1H, J 2.0, pyridinone-H), 6.40 (s, 1H, pyridinone-H). ¹³C NMR (CDCl₃) δ 17.5, 37.1, 115.1, 115.7, 123.5, 136.8, 157.1. **HRMS** (ESI-TOF) *m/z* 139.0876 [M+H]⁺; calcd. for $C_7H_{11}N_2O^+$ 139.0866 [M+H]⁺.

4.1.4. 3-Amino-1-(2-methoxyethyl)-5-methylpyridin-2(1H)-one (3b)

Nitro compound **2b** (212 mg, 0.999 mmol) was reduced according to general synthetic procedure B to give **3b** as a brown oil (182 mg, 100%). **R$_F$** (DCM:CH_3OH = 9:1) 0.57. ¹H NMR (CDCl₃) δ 1.83 (s, 3H, pyridinone-CH_3), 3.15 (s, 3H, OCH_3), 3.52 (t, 2H, J 5.0, CH_2CH_2), 3.93 (t, 2H, J 5.0, CH_2CH_2), 4.18 (br s, 2H, NH_2), 6.26 (d, 1H, J 1.5, pyridinone-H), 6.39 (s, 1H, pyridinone-H). ¹³C NMR (CDCl₃) δ 17.4, 49.3, 58.6, 70.2, 115.0, 115.1, 123.5, 136.8, 156.5. **HRMS** (ESI-TOF) *m/z* 205.0947 [M+Na]⁺; calcd. for $C_9H_{14}N_2NaO_2^+$ 205.0947 [M+Na]⁺.

4.1.5. Methyl 4-chloro-5-methylthieno[2,3-d]pyrimidine-6-carboxylate (5)

To a suspension of methyl 5-methyl-4-oxo-3,4-dihydrothieno[2,3-d]pyrimidine-6-carboxylate (**4**, 4.48 g, 20.0 mmol) in $SOCl_2$ (40.0 mL, 548 mmol) was added DMF (800 μL, 10.3 mmol). The reaction mixture was heated at reflux under N_2 for 2 h, cooled down to room temperature, stirred overnight and concentrated under reduced pressure. The residue was purified by Biotage® FlashMaster Personal⁺ flash chromatography (silica gel, DCM ramping to DCM:EtOAc = 98:2) to give **5** as a white solid (4.30 g, 89%). **R$_F$** (DCM:EtOAc = 98:2) 0.57. **m.p.** 141–142 °C. ¹H NMR (CDCl₃) δ 2.97 (s, 3H, thiophene-CH_3), 3.91 (s, 3H, $COOCH_3$), 8.79 (s, 1H, pyrimidine-H). ¹³C NMR (CDCl₃) δ 15.8, 52.8, 127.9, 128.8, 139.2, 154.2, 157.3, 162.4, 169.1. **HRMS** (ESI-TOF) *m/z* 243.0004 [M(³⁵Cl)+H]⁺, 244.9975 [M(³⁷Cl)+H]⁺; calcd. for $C_9H_8ClN_2O_2S^+$ 242.9990 [M(³⁵Cl)+H]⁺, 244.9960 [M(³⁷Cl)+H]⁺.

4.1.6. Methyl 4-((1,5-dimethyl-2-oxo-1,2-dihydropyridin-3-yl) amino)-5-methylthieno[2,3-d]pyrimidine-6-carboxylate (6a)

Chloride **5** (485 mg, 2.00 mmol) and amine **3a** (273 mg, 1.98 mmol) were subjected to general synthetic procedure C. The residue was purified by Biotage® FlashMaster Personal⁺ flash chromatography (silica gel, DCM ramping to DCM:CH_3OH = 99:1)

to give **6a** as a yellow solid (587 mg, 86%). R_F (DCM:CH_3OH = 95:5) 0.45. **m.p.** 270–272 °C. ^{1}**H NMR** (CDCl$_3$) δ 2.20 (s, 3H, pyridinone-CH$_3$), 3.21 (s, 3H, thiophene-CH$_3$), 3.63 (s, 3H, NCH$_3$), 3.93 (s, 3H, COOCH$_3$), 6.82 (s, 1H, pyridinone-H), 8.69 (s, 2H, pyridinone-H & pyrimidine-H), 9.49 (br s, 1H, NH). ^{13}**C NMR** (CDCl$_3$) δ 15.9, 18.2, 37.9, 52.5, 116.3, 118.6, 123.7, 124.9, 127.5, 129.3, 138.3, 155.3, 156.3, 157.6, 163.3, 167.3. **HRMS** (ESI-TOF) *m/z* 345.1033 [M+H]$^+$; calcd. for C$_{16}$H$_{17}$N$_4$O$_3$S$^+$ 345.1016 [M+H]$^+$. **Anal. RP-HPLC** Method A: t_R 12.76 min, purity >98%; Method B: t_R 11.18 min, purity >97%.

4.1.7. Methyl 4-((1-(2-methoxyethyl)-5-methyl-2-oxo-1,2-dihydropyridin-3-yl)amino)-5-methylthieno[2,3-d]pyrimidine-6-carboxylate (6b)

Chloride **5** (243 mg, 1.00 mmol) and amine **3b** (182 mg, 0.999 mmol) were subjected to general synthetic procedure C to give **6b** as a yellow solid (210 mg, 54%). R_F (DCM:CH_3OH = 95:5) 0.58. **m.p.** 216 °C. ^{1}**H NMR** (CDCl$_3$) δ 2.18 (s, 3H, pyridinone-CH$_3$), 3.18 (s, 3H, thiophene-CH$_3$), 3.33 (s, 3H, CH$_2$OCH$_3$), 3.70 (t, 2H, *J* 4.5, CH$_2$CH$_2$), 3.91 (s, 3H, COOCH$_3$), 4.16 (t, 2H, *J* 4.5, CH$_2$CH$_2$), 6.84 (s, 1H, pyridinone-H), 8.65 (s, 1H, pyrimidine-H), 8.69 (s, 1H, pyridinone-H), 9.29 (s, 1H, NH). ^{13}**C NMR** (CDCl$_3$) δ 15.9, 18.3, 50.4, 52.5, 59.2, 70.4, 115.6, 118.5, 123.5, 125.2, 128.1, 129.1, 138.4, 155.3, 156.3, 157.2, 163.2, 167.4. **HRMS** (ESI-TOF) *m/z* 389.1267 [M+H]$^+$; calcd. for C$_{18}$H$_{21}$N$_4$O$_4$S$^+$ 389.1278 [M+H]$^+$. **Anal. RP-HPLC** Method A: t_R 11.34 min, purity >99%; Method B: t_R 9.97 min, purity >98%.

4.1.8. 4-((1,5-Dimethyl-2-oxo-1,2-dihydropyridin-3-yl)amino)-5-methylthieno[2,3-d]pyrimidine-6-carboxylic acid (7a)

Ester **6a** (751 mg, 2.18 mmol) was hydrolysed using general synthetic procedure D to give **7a** as a greenish solid (720 mg, 100%). **m.p.** > 300 °C. ^{1}**H NMR** (DMSO-d_6) δ 2.12 (s, 3H, pyridinone-CH$_3$), 3.09 (s, 3H, thiophene-CH$_3$), 3.54 (s, 3H, NCH$_3$), 7.23 (s, 1H, pyridinone-H), 8.59 (d, 1H, *J* 2.0, pyridinone-H), 8.67 (s, 1H, pyrimidine-H), 9.28 (s, 1H, NH) (one carboxylic acid proton signal (COOH) not observed). ^{13}**C NMR** (DMSO-d_6) δ 15.0, 17.5, 37.2, 114.2, 118.3, 123.7, 128.3, 128.7, 154.9, 155.6, 156.6, 163.8, 166.0 (two carbon signals overlapping or obscured). **HRMS** (ESI-TOF) *m/z* 331.0871 [M+H]$^+$; calcd. for C$_{15}$H$_{15}$N$_4$O$_3$S$^+$ 331.0859 [M+H]$^+$. **Anal. RP-HPLC** Method A: t_R 11.89 min, purity >98%; Method B: t_R 9.56 min, purity >98%.

4.1.9. 4-((1-(2-Methoxyethyl)-5-methyl-2-oxo-1,2-dihydropyridin-3-yl)amino)-5-methylthieno[2,3-d]pyrimidine-6-carboxylic acid (7b)

Ester **6b** (155 mg, 0.399 mmol) was hydrolysed using general synthetic procedure D to give **7b** as a greenish solid (125 mg, 84%). **m.p.** 295–296 °C. ^{1}**H NMR** (DMSO-d_6) δ 2.11 (s, 3H, pyridinone-CH$_3$), 3.05 (s, 3H, thiophene-CH$_3$), 3.26 (s, 3H, OCH$_3$), 3.63 (t, 2H, *J* 5.5, CH$_2$CH$_2$), 4.13 (t, 2H, *J* 5.5, CH$_2$CH$_2$), 7.16 (s, 1H, pyridinone-H), 8.55 (d, 1H, *J* 1.5, pyridinone-H), 8.64 (s, 1H, pyrimidine-H), 9.20 (s, 1H, NH) (one carboxylic acid proton signal (COOH) not observed). ^{13}**C NMR** (DMSO-d_6) δ 15.1, 17.6, 49.0, 58.1, 69.4, 114.0, 118.2, 124.1, 128.3, 128.7, 137.1, 155.0, 155.6, 156.3, 163.8, 166.1 (one carbon signal overlapping or obscured). **HRMS** (ESI-TOF) *m/z* 375.1118 [M+H]$^+$; calcd. for C$_{17}$H$_{19}$N$_4$O$_4$S$^+$ 375.1122 [M+H]$^+$. **Anal. RP-HPLC** Method A: t_R 10.85 min, purity >99%; Method B: t_R 8.62 min, purity >99%.

4.1.10. 4-((1,5-Dimethyl-2-oxo-1,2-dihydropyridin-3-yl)amino)-5-methylthieno[2,3-d]pyrimidine-6-carboxamide (8a)

Carboxylic acid **7a** (83.0 mg, 0.251 mmol) and NH$_3$ (0.5 M in 1,4-dioxane, 2.50 mL, 1.25 mmol) were coupled using general synthetic procedure E to give **8a** as an off-white solid (66.0 mg, 80%). **m.p.** > 300 °C. ^{1}**H NMR** (DMSO-d_6) δ 2.12 (s, 3H, pyridinone-CH$_3$), 2.94 (s, 3H, thiophene-CH$_3$), 3.54 (s, 3H, NCH$_3$), 7.23 (s, 1H, pyridinone-H), 7.86 (br d, 2H, *J* 59.0, CONH$_2$), 8.59 (d, 1H, *J* 1.5, pyridinone-H), 8.66 (s, 1H, pyrimidine-H), 9.23 (s, 1H, pyridinone-NH-pyrimidine). ^{13}**C NMR** (DMSO-d_6) δ 15.2, 17.0, 36.5, 113.8, 117.5, 123.4, 128.1, 129.1, 130.2, 153.8, 155.1, 156.5, 163.5, 165.1 (one carbon signal overlapping or obscured). **HRMS** (ESI-TOF) *m/z* 352.0838 [M+Na]$^+$; calcd. for C$_{15}$H$_{15}$N$_5$NaO$_2$S$^+$ 352.0839 [M+Na]$^+$. **Anal. RP-HPLC** Method A: t_R 10.88 min, purity >98%; Method B: t_R 8.77 min, purity >98%.

4.1.11. 4-((1,5-Dimethyl-2-oxo-1,2-dihydropyridin-3-yl)amino)-N,5-dimethylthieno[2,3-d]pyrimidine-6-carboxamide (8b)

Carboxylic acid **7a** (83.0 mg, 0.251 mmol) and methylamine hydrochloride (84.0 mg, 1.24 mmol) were coupled using general synthetic procedure E to give **8b** as a beige solid (31.0 mg, 36%). **m.p.** > 300 °C. ^{1}**H NMR** (DMSO-d_6) δ 2.12 (d, 3H, *J* 0.5, pyridinone-CH$_3$), 2.80 (d, 3H, *J* 4.5, CONHCH$_3$), 2.91 (s, 3H, thiophene-CH$_3$), 3.54 (s, 3H, NCH$_3$), 7.23 (dd, 1H, *J* 2.0 & 1.0, pyridinone-H), 8.42 (q, 1H, *J* 4.5, CONHCH$_3$), 8.59 (d, 1H, *J* 2.0, pyridinone-H), 8.66 (s, 1H, pyrimidine-H), 9.22 (s, 1H, pyridinone-NH-pyrimidine). ^{13}**C NMR** (DMSO-d_6) δ 15.7, 17.5, 26.5, 37.2, 114.2, 117.7, 123.6, 128.3, 128.6, 128.9, 130.4, 154.3, 155.3, 156.6, 162.5, 165.2. **HRMS** (ESI-TOF) *m/z* 344.1167 [M+H]$^+$; calcd. for C$_{16}$H$_{18}$N$_5$O$_2$S$^+$ 344.1176 [M+H]$^+$. **Anal. RP-HPLC** Method A: t_R 11.15 min, purity >97%; Method B: t_R 9.11 min, purity >97%.

4.1.12. 4-((1,5-Dimethyl-2-oxo-1,2-dihydropyridin-3-yl)amino)-N-ethyl-5-methylthieno[2,3-d]pyrimidine-6-carboxamide (8c)

Carboxylic acid **7a** (83.0 mg, 0.251 mmol) and ethylamine (2.0 M in THF, 625 μL, 1.25 mmol) were coupled using general synthetic procedure E to give **8c** as a beige solid (59.0 mg, 66%). **m.p.** 284–286 °C. ^{1}**H NMR** (DMSO-d_6) δ 1.14 (t, 3H, *J* 7.5, NHCH$_2$CH$_3$), 2.12 (s, 3H, pyridinone-CH$_3$), 2.90 (s, 3H, thiophene-CH$_3$), 3.26–3.32 (m, 2H, NHCH$_2$CH$_3$), 3.54 (s, 3H, NCH$_3$), 7.23 (d, 1H, *J* 1.0, pyridinone-H), 8.51 (t, 1H, *J* 5.5, NHCH$_2$CH$_3$), 8.59 (d, 1H, *J* 2.5, pyridinone-H), 8.66 (s, 1H, pyrimidine-H), 9.22 (s, 1H, pyridinone-NH-pyrimidine). ^{13}**C NMR** (DMSO-d_6) δ 14.7, 15.8, 17.6, 34.4, 37.2, 114.3, 117.7, 123.6, 128.3, 128.6, 129.3, 130.2, 154.3, 155.3, 156.7, 161.8, 165.2. **HRMS** (ESI-TOF) *m/z* 358.1329 [M+H]$^+$; calcd. for C$_{17}$H$_{20}$N$_5$O$_2$S$^+$ 358.1332 [M+H]$^+$. **Anal. RP-HPLC** Method A: t_R 11.44 min, purity >98%; Method B: t_R 9.57 min, purity >99%.

4.1.13. 4-((1,5-Dimethyl-2-oxo-1,2-dihydropyridin-3-yl)amino)-N-(2-methoxyethyl)-5-methylthieno[2,3-d]pyrimidine-6-carboxamide (8d)

Carboxylic acid **7a** (74 mg, 0.22 mmol) and 2-methoxypropylamine (96 μL, 1.1 mmol) were coupled using general synthetic procedure E to give **8d** as a pale yellow solid (50 mg, 58%). **m.p.** 245–246 °C. ^{1}**H NMR** (DMSO-d_6) δ 2.12 (s, 3H, pyridinone-CH$_3$), 2.90 (s, 3H, thiophene-CH$_3$), 3.30 (s, 3H, OCH$_3$), 3.41–3.45 (m, 2H, CH$_2$CH$_2$), 3.47–3.50 (m, 2H, CH$_2$CH$_2$), 3.54 (s, 3H, NCH$_3$), 7.23 (d, 1H, *J* 1.0, pyridinone-H), 8.55 (t, 1H, *J* 5.5, CONHCH$_2$), 8.59 (d, 1H, *J* 2.0, pyridinone-H), 8.66 (s, 1H, pyrimidine-H), 9.23 (s, 1H, pyridinone-NH-pyrimidine). ^{13}**C NMR** (DMSO-d_6) δ 15.8, 17.5, 37.1, 58.0, 70.2, 114.2, 117.6, 123.5, 128.3, 128.6, 129.2, 130.3, 154.3, 155.2, 156.6, 162.1, 165.3 (one carbon signal overlapping or obscured). **HRMS** (ESI-TOF) *m/z* 388.1446 [M+H]$^+$; calcd. for C$_{18}$H$_{22}$N$_5$O$_3$S$^+$ 388.1438 [M+H]$^+$. **Anal. RP-HPLC** Method A: t_R 11.30 min, purity >99%; Method B: t_R 9.30 min, purity >99%.

4.1.14. 4-((1,5-Dimethyl-2-oxo-1,2-dihydropyridin-3-yl)amino)-N-(3-methoxypropyl)-5-methylthieno[2,3-d]pyrimidine-6-carboxamide (8e)

Carboxylic acid **7a** (132 mg, 0.400 mmol) and 3-methoxypropylamine (204 μL, 2.00 mmol) were coupled using general synthetic procedure E to give **8e** as a pale yellow solid (60.0 mg, 37%). **m.p.** 230–231 °C. ^{1}**H NMR** (DMSO-d_6) δ 1.75–1.81

(m, 2H, CH₂C*H*₂CH₂), 2.12 (s, 3H, pyridinone-CH₃), 2.90 (s, 3H, thiophene-CH₃), 3.26 (s, 3H, OCH₃), 3.29–3.34 (m, 2H, NHC*H*₂CH₂), 3.40 (t, 2H, *J* 6.5, CH₂C*H*₂O), 3.53 (s, 3H, NCH₃), 7.22 (d, 1H, *J* 1.0, pyridinone-H), 8.49 (t, 1H, *J* 5.5, CONH*CH*₂), 8.58 (d, 1H, *J* 2.0, pyridinone-H), 8.65 (s, 1H, pyrimidine-H), 9.21 (s, 1H, pyridinone-NH-pyrimidine). ¹³C NMR (DMSO-*d*₆) δ 15.8, 17.5, 29.0, 36.9, 37.1, 58.0, 69.7, 114.2, 117.6, 123.5, 128.3, 128.6, 129.2, 130.1, 154.3, 155.2, 156.6, 162.0, 165.2. HRMS (ESI-TOF) *m/z* 402.1577 [M+H]⁺; calcd. for C₁₉H₂₄N₅O₃S⁺ 402.1594 [M+H]⁺. Anal. RP-HPLC Method A: *t*ᴿ 11.56 min, purity >96%; Method B: *t*ᴿ 9.60 min, purity >96%.

4.1.15. 4-((1-(2-Methoxyethyl)-5-methyl-2-oxo-1,2-dihydropyridin-3-yl)amino)-5-methylthieno[2,3-d]pyrimidine-6-carboxamide (8f)

Carboxylic acid 7b (75 mg, 0.20 mmol) and NH₃ (0.5 M in 1,4-dioxane, 2.0 mL, 1.0 mmol) were coupled using general synthetic procedure E to give 8f as a yellowish solid (49 mg, 66%). m.p. 263–264 °C. ¹H NMR (DMSO-*d*₆) δ 2.12 (s, 3H, pyridinone-CH₃), 2.93 (s, 3H, thiophene-CH₃), 3.25 (s, 3H, OCH₃), 3.64 (t, 2H, *J* 5.5, C*H*₂CH₂), 4.14 (t, 2H, *J* 5.5, CH₂C*H*₂), 7.17 (s, 1H, pyridinone-H), 7.86 (br d, 2H, *J* 56.0, CONH₂), 8.60 (d, 1H, *J* 2.0, pyridinone-H), 8.65 (s, 1H, pyrimidine-H), 9.20 (s, 1H, pyridinone-NH-pyrimidine). ¹³C NMR (DMSO-*d*₆) δ 15.3, 17.1, 48.5, 57.7, 69.2, 113.6, 117.5, 123.6, 127.9, 128.1, 129.1, 130.2, 153.8, 155.1, 156.2, 163.5, 165.1. HRMS (ESI-TOF) *m/z* 374.1263 [M+H]⁺; calcd. for C₁₇H₂₀N₅O₃S⁺ 374.1281 [M+H]⁺. Anal. RP-HPLC Method A: *t*ᴿ 10.04 min, purity >98%; Method B: *t*ᴿ 7.90 min, purity >97%.

4.1.16. 1-Methyl-5-nitropyridin-2(1H)-one (10)

5-Nitropyridin-2(1*H*)-one (9, 700 mg, 5.00 mmol) and iodo-methane (467 μL, 7.50 mmol) were reacted using general synthetic procedure A to give 10 as a pale yellow solid (763 mg, 99%). *R*ꜰ (DCM:CH₃OH = 98:2) 0.41. m.p. 173–174 °C. ¹H NMR (CDCl₃) δ 3.65 (s, 3H, NCH₃), 6.55 (d, 1H, *J* 10.0, pyridinone-H), 8.08 (dd, 1H, *J* 10.0 & 3.0, pyridinone-H), 8.64 (d, 1H, *J* 3.0, pyridinone-H). ¹³C NMR (CDCl₃) δ 38.9, 119.3, 130.6, 133.4, 140.2, 162.0. HRMS (ESI-TOF) *m/z* 155.0453 [M+H]⁺; calcd. for C₆H₇N₂O₃⁺ 155.0451 [M+H]⁺.

4.1.17. Methyl 5-methyl-4-((1-methyl-6-oxo-1,6-dihydropyridin-3-yl)amino)thieno[2,3-d]pyrimidine-6-carboxylate (12)

Nitro compound 10 (308 mg, 2.00 mmol) was reduced according to general synthetic procedure B to give 11 as a dark green semi-solid. The semi-solid and chloride 5 (242 mg, 0.997 mmol) were subjected to general synthetic procedure C to give 12 as a yellow solid (225 mg, 68%). *R*ꜰ (DCM:CH₃OH = 95:5) 0.29. m.p. 260 °C. ¹H NMR (CDCl₃) δ 3.09 (s, 3H, thiophene-CH₃), 3.60 (s, 3H, NCH₃), 3.94 (s, 3H, COOCH₃), 6.65 (d, 1H, *J* 9.5, pyridinone-H), 7.02 (br s, 1H, NH), 7.37 (dd, 1H, *J* 9.5 & 3.0, pyridinone-H), 7.89 (d, 1H, *J* 3.0, pyridinone-H), 8.55 (s, 1H, pyrimidine-H). ¹³C NMR (CDCl₃) δ 16.0, 38.1, 52.6, 117.4, 118.1, 121.0, 124.1, 133.8, 137.0, 138.4, 155.5, 157.8, 161.7, 163.2, 167.9. HRMS (ESI-TOF) *m/z* 331.0840 [M+H]⁺; calcd. for C₁₅H₁₅N₄O₃S⁺ 331.0859 [M+H]⁺. Anal. RP-HPLC Method A: *t*ᴿ 7.54 min, purity >96%; Method B: *t*ᴿ 9.11 min, purity >96%.

4.1.18. 5-Methyl-4-((1-methyl-6-oxo-1,6-dihydropyridin-3-yl)amino)thieno[2,3-d]pyrimidine-6-carboxylic acid (13)

To a suspension of 12 (225 mg, 0.681 mmol) in CH₃OH (15 mL) was added 2 M NaOH (4.50 mL, 9.00 mmol). The reaction mixture was stirred at room temperature for 48 h and filtered, the solids were washed with CH₃OH (5 mL). The filtrate and washing were combined, acidified with 2 M HCl to pH 3. The precipitate was filtered, washed with H₂O (3 × 25 mL), and dried under reduced pressure to give 13 as a white solid (190 mg, 88%). m.p. > 300 °C. ¹H NMR (DMSO-*d*₆) δ 2.99 (s, 3H, thiophene-CH₃), 3.45 (s, 3H, NCH₃), 6.43 (d, 1H, *J* 9.5, pyridinone-H), 7.54 (dd, 1H, *J* 9.5 & 3.0,

pyridinone-H), 7.86 (d, 1H, *J* 3.0, pyridinone-H), 8.40 (s, 1H, NH), 8.41 (s, 1H, pyrimidine-H) (one carboxylic acid proton signal (COOH) not observed). ¹³C NMR (DMSO-*d*₆) δ 15.5, 37.0, 117.3, 118.2, 118.3, 123.1, 135.8, 138.6, 140.9, 155.1, 158.0, 160.7, 163.9, 166.7. HRMS (ESI-TOF) *m/z* 317.0684 [M+H]⁺; calcd. for C₁₄H₁₃N₄O₃S⁺ 317.0703 [M+H]⁺. Anal. RP-HPLC Method A: *t*ᴿ 8.15 min, purity >98%; Method B: *t*ᴿ 6.57 min, purity >99%.

4.1.19. 5-Methyl-4-((1-methyl-6-oxo-1,6-dihydropyridin-3-yl)amino)thieno[2,3-d]pyrimidine-6-carboxamide (14)

Carboxylic acid 13 (111 mg, 0.351 mmol) and NH₃ (0.5 M in 1,4-dioxane, 3.50 mL, 1.75 mmol) were coupled using general synthetic procedure E to give 14 as a white solid (60.0 mg, 54%). m.p. > 300 °C. ¹H NMR (DMSO-*d*₆) δ 2.85 (s, 3H, thiophene-CH₃), 3.45 (s, 3H, NCH₃), 6.42 (d, 1H, *J* 9.5, pyridinone-H), 7.53 (dd, 1H, *J* 9.5 & 3.0, pyridinone-H), 7.77 (br d, 2H, *J* 31.0, CONH₂), 7.86 (d, 1H, *J* 2.5, pyridinone-H), 8.31 (s, 1H, pyridinone-NH-pyrimidine), 8.38 (s, 1H, pyrimidine-H). ¹³C NMR (DMSO-*d*₆) δ 15.9, 36.9, 116.9, 118.2, 127.8, 132.1, 135.7, 141.0, 154.3, 157.7, 160.6, 164.0, 165.7 (one carbon signal overlapping or obscured). HRMS (ESI-TOF) *m/z* 316.0880 [M+H]⁺; calcd. for C₁₄H₁₄N₅O₂S⁺ 316.0863 [M+H]⁺. Anal. RP-HPLC Method A: *t*ᴿ 8.65 min, purity >99%; Method B: *t*ᴿ 7.04 min, purity >99%.

4.2. Computational methods

An in-house Mnk2 DFD-in conformation that was modelled using homology modelling and molecular dynamics simulations was used for the docking [29]. The docking grid was generated to encompass the ATP binding site. Schrödinger's induced fit docking protocol [30,31] was used to dock 7a, while allowing residues in a 5 Å radius to be flexible. The top 10 poses were visually inspected to reveal that the three best scoring binding modes are highly similar. Subsequently, the best scoring mode was selected to rationalise the binding affinity of 7a for Mnk2.

4.3. Biology

4.3.1. ADP-Glo™ kinase assay

The luminescent ADP-Glo™ assay kits were purchased from Promega (Madison, WI, USA). Serial dilution of compounds 6–8 and 10–12 with a dilution factor of 1:3 was carried out to give 8 concentrations ranging from 10 μM to 4.5 nM with 0.5% DMSO. Each compound was added to the kinase reaction containing 1 × kinase reaction buffer, 0.1 mg/mL BSA, Milli-Q H₂O, eIF4E peptide substrate (custom synthesis, Resolving Images, Thomas-town, Vic) and Mnk (Merck Millipore, Kilsyth, Vic) in a total assay volume of 15 μL and incubated for 10 min. The kinase reaction was initiated by addition of ATP, incubated at 30 °C for 45 min and stopped with ADP Glo™ reagent (15 μL), followed by incubation in the dark at room temperature for 40 min. Kinase detection reagent (30 μL) was added. The mixture was further incubated for 40 min before reading in an EnVision multi-label plate reader (Perki-nElmer, Beaconsfield, Buckinghamshire, UK). Positive and negative controls were performed with 0.5% DMSO in the absence and presence of Mnk respectively.

4.3.2. Kinase panel assay

Percentages of residual kinase activity upon treatment with 7a, 7b or 8e at the concentration of 10 μM were determined using the Millipore KinaseProfiler services, and ATP concentrations used were within 15 μM of K_m values.

4.3.3. Cell culture

MV-4-11 cells were provided by Professor Richard D'Andrea (University of South Australia) and maintained in Roswell Park

Memorial Institute medium (RPMI)-1640 with 10% fetal bovine serum (FBS).

4.3.4. Cell viability assay

Resazurin assays were performed on MV-4-11 cells as previously reported [18]. Cells were seeded at 5×10^3 cells/well into 96-well plates and incubated at 37 °C, 5% CO_2 overnight. Each compound was diluted from a 2 or 10 mM stock solution to prepare a five-fold dilution series in 100 μL of cell medium, added to cells (in triplicates), and incubated at 37 °C, 5% CO_2 for 72 h. Resazurin (Sigma–Aldrich) was made up as a stock of 0.1 mg/mL in cell medium and filter-sterilised. The resazurin solution was added at 20 μL/well and incubated in the dark at 37 °C, 5% CO_2 for 4 h. The plate was left at room temperature for 10–15 min, and absorbance was measured at 585 nm using an EnVision multi-label plate reader (PerkinElmer, Beaconsfield, Buckinghamshire, UK). Compound concentrations required to inhibit 50% of cell growth (GI_{50}) were calculated using non-linear regression analysis.

4.3.5. Caspase-3/7 assay

Activity of caspase-3/7 was measured using the Apo-ONE Homogeneous Caspase-3/7 kit (G7790 Promega, Madison, WI, USA) according to manufacturer instruction and analysed using an EnVision multi-label plate reader (PerkinElmer, Beaconsfield, Buckinghamshire, UK).

4.3.6. Cell cycle analysis and apoptosis detection

Cell cycle analysis and apoptosis detection were performed with flow cytometry as described previously [18]. Briefly, MV-4-11 cells were seeded at 8×10^4 and incubated at 37 °C, 5% CO_2 overnight. After treatment with each compound for 24 h, cell pellets were collected and centrifuged ($300 \times g$, 5 min). For cell cycle analysis, cell pellets were fixed with 70% ethanol on ice for 15 min and collected again. The collected pellets were incubated with propidium iodide (PI) staining solution (50 μg/mL PI, 0.1 mg/mL RNase A, 0.05% Triton X-100) at room temperature for 1 h and analysed by a Gallios flow cytometer (Beckman Coulter, Brea, CA, USA). Apoptosis detection was carried out with the FITC Annexin-V/PI commercial kit (Becton Dickenson, Franklin Lakes, NJ, USA) following the manufacturer protocol. The samples were analysed by fluorescence-activated cell sorting (FACS) with a Gallios flow cytometer (Beckman Coulter, Brea, CA, USA) within 1 h after staining. Data were analysed using Kaluza v1.2 (Beckman Coulter).

4.3.7. Western blots

Western blotting was performed as described previously [32,33]. Antibodies used were Mnk1, eIF4E, p-eIF4E^{Ser209}, Bcl-2, Mcl-1, cyclin D1, PARP, cleaved PARP and β-actin. Both anti-mouse and anti-rabbit immunoglobulin G (IgG) horseradish peroxidase-conjugated antibodies (Dako, Glostrap, Denmark) were used as secondary antibodies. Enhanced Chemiluminescence (ECL) reagents (GE Life Sciences) were used for Western blotting detection.

Acknowledgements

Appendix A. Supplementary data

Supplementary data related to this article can be found at http://dx.doi.org/10.1016/j.ejmech.2015.03.032.

References

[1] J.P.C. Le Quesne, K.A. Spriggs, M. Bushell, A.E. Willis, Dysregulation of protein synthesis and disease, J. Pathol. 220 (2010) 140–151.

[2] V.M. Pain, Initiation of protein synthesis in eukaryotic cells, Eur. J. Biochem. 236 (1996) 747–771.

[3] A.J. Waskiewicz, A. Flynn, C.G. Proud, J.A. Cooper, Mitogen-activated protein kinases activate the serine/threonine kinases Mnk1 and Mnk2, EMBO J. 16 (1997) 1909–1920.

[4] J. Hou, F. Lam, C.G. Proud, S. Wang, Targeting Mnks for cancer therapy, Oncotarget 3 (2012) 118–131.

[5] S. Diab, M. Kumarasiri, M. Yu, T. Teo, C. Proud, R. Milne, S. Wang, MAP kinase-interacting kinases—emerging targets against cancer, Chem. Biol. 21 (2014) 441–452.

[6] L. Furic, L. Rong, O. Larsson, I.H. Koumakpayi, K. Yoshida, A. Brueschke, E. Petroulakis, N. Robichaud, M. Pollak, L.A. Gaboury, P.P. Pandolfi, F. Saad, N. Sonenberg, eIF4E phosphorylation promotes tumorigenesis and is associated with prostate cancer progression, Proc. Natl. Acad. Sci. U. S. A. 107 (2010) 14134–14139.

[7] T. Ueda, M. Sasaki, A.J. Elia, I.I.C. Chio, K. Hamada, R. Fukunaga, T.W. Mak, Combined deficiency for MAP kinase-interacting kinase 1 and 2 (Mnk1 and Mnk2) delays tumor development, Proc. Natl. Acad. Sci. U. S. A. 107 (2010) 13984–13990.

[8] H.G. Wendel, R.L. Silva, A. Malina, J.R. Mills, H. Zhu, T. Ueda, R. Watanabe-Fukunaga, R. Fukunaga, J. Teruya-Feldstein, J. Pelletier, S.W. Lowe, Dissecting eIF4E action in tumorigenesis, Genes. Dev. 21 (2007) 3232–3237.

[9] T. Ueda, R. Watanabe-Fukunaga, H. Fukuyama, S. Nagata, R. Fukunaga, Mnk2 and Mnk1 are essential for constitutive and inducible phosphorylation of eukaryotic initiation factor 4E but not for cell growth or development, Mol. Cell. Biol. 24 (2004) 6539–6549.

[10] R. Fukunaga, T. Hunter, MNK1, a new MAP kinase-activated protein kinase, isolated by a novel expression screening method for identifying protein kinase substrates, EMBO J. 16 (1997) 1921–1933.

[11] C. Tschopp, U. Knauf, M. Brauchle, M. Zurini, P. Ramage, D. Glueck, L. New, J. Han, H. Gram, Phosphorylation of eIF4E on Ser 209 in response to mitogenic and inflammatory stimuli is faithfully detected by specific antibodies, Mol. Cell. Biol. Res. Commun. 3 (2000) 205–211.

[12] M. Buxade, J. Parra-Palau, C. Proud, The Mnks: MAP kinase-interacting kinases (MAP kinase signal-integrating kinases), Front. Biosci. 13 (2008) 5359–5374.

[13] U. Knauf, C. Tschopp, H. Gram, Negative regulation of protein translation by mitogen-activated protein kinase-interacting kinases 1 and 2, Mol. Cell. Biol. 21 (2001) 5500–5511.

[14] B.W. Konicek, J.R. Stephens, A.M. McNulty, N. Robichaud, R.B. Peery, C.A. Dumstorf, M.S. Dowless, P.W. Iversen, S. Parsons, K.E. Ellis, D.J. McCann, J. Pelletier, L. Furic, J.M. Yingling, L.F. Stancato, N. Sonenberg, J.R. Graff, Therapeutic inhibition of MAP kinase interacting kinase blocks eukaryotic initiation factor 4E phosphorylation and suppresses outgrowth of experimental lung metastases, Cancer Res. 71 (2011) 1849–1857.

[15] R. Jogireddy, P.-Y. Dakas, G. Valot, S. Barluenga, N. Winssinger, Synthesis of a resorcylic acid lactone (RAL) library using fluorous-mixture synthesis and profile of its selectivity against a panel of kinases, Chem. Eur. J. 15 (2009) 11498–11506.

[16] S. Barluenga, R. Jogireddy, G.K. Koripelly, N. Winssinger, In vivo efficacy of natural product-inspired irreversible kinase inhibitors, ChemBioChem 11 (2010) 1692–1699.

[17] J. Xu, A. Chen, J. Joy, V.J. Xavier, E.H. Ong, J. Hill, C.L. Chai, Rational design of resorcylic acid lactone analogues as covalent MNK1/2 kinase inhibitors by tuning the reactivity of an enamide michael acceptor, ChemMedChem 8 (2013) 1483–1494.

[18] S. Diab, T. Teo, M. Kumarasiri, P. Li, M. Yu, F. Lam, S.K.C. Basnet, M.J. Sykes, H. Albrecht, R. Milne, S. Wang, Discovery of 5-(2-(phenylamino)pyrimidin-4-yl)thiazol-2(3H)-one derivatives as potent Mnk2 inhibitors: synthesis, SAR analysis and biological evaluation, ChemMedChem 9 (2014) 962–972.

[19] R. Jauch, M.K. Cho, S. Jakel, C. Netter, K. Schreiter, B. Aicher, M. Zweckstetter, H. Jackle, M.C. Wahl, Mitogen-activated protein kinases interacting kinases are autoinhibited by a reprogrammed activation segment, EMBO J. 25 (2006) 4020–4032.

[20] R. Jauch, S. Jakel, C. Netter, K. Schreiter, B. Aicher, H. Jackle, M.C. Wahl, Crystal structures of the Mnk2 kinase domain reveal an inhibitory conformation and a zinc binding site, Structure 13 (2005) 1559–1568.

[21] J. Hou, T. Teo, M.J. Sykes, S. Wang, Insights into the importance of DFD-motif and insertion I1 in stabilizing the DFD-out conformation of Mnk2 kinase, ACS Med. Chem. Lett. 4 (2013) 736–741.

[22] T. Teo, Y. Yang, M. Yu, S.K. Basnet, T. Gillam, J. Hou, F. Lam, R.M. Schmid, M. Kumarasiri, S. Diab, H. Albrecht, M.J. Sykes, S. Wang, An integrated approach for discovery of highly potent and selective Mnk inhibitors: screening, synthesis and biological evaluations, 2015 (manuscript revised).

[23] I. Topisirovic, M.L. Guzman, M.J. McConnell, J.D. Licht, B. Culjkovic, S.J. Neering, C.T. Jordan, K.L.B. Borden, Aberrant eukaryotic translation initiation factor 4E-dependent mRNA transport impedes hematopoietic differentiation and contributes to leukemogenesis, Mol. Cell. Biol. 23 (2003) 8992–9002.

[24] J.K. Altman, A. Szilard, B.W. Konicek, P.W. Iversen, B. Kroczynska, H. Glaser, A. Sassano, E. Vakana, J.R. Graff, L.C. Platanias, Inhibition of Mnk kinase activity by cercosporamide and suppressive effects on acute myeloid leukemia

precursors, Blood 121 (2013) 3675—3681.

[25] S. Lim, T.Y. Saw, M. Zhang, M.R. Janes, K. Nacro, J. Hill, A.Q. Lim, C.-T. Chang, D.A. Fruman, D.A. Rizzieri, Targeting of the MNK—eIF4E axis in blast crisis chronic myeloid leukemia inhibits leukemia stem cell function, Proc. Natl. Acad. Sci. 110 (2013) E2298—E2307.

[26] M. Koresawa, T. Okabe, High-throughput screening with quantitation of ATP consumption: a universal non-radioisotope, homogeneous assay for protein kinase, Assay. Drug Dev. Technol. 2 (2004) 153—160.

[27] J.T. Reilly, Class III receptor tyrosine kinases: role in leukaemogenesis, Br. J. Haematol. 116 (2002) 744—757.

[28] H. Quentmeier, J. Reinhardt, M. Zaborski, H.G. Drexler, FLT3 mutations in acute myeloid leukemia cell lines, Leukemia 17 (2003) 120—124.

[29] M. Kumarasiri, T. Teo, S. Wang, Dynamical insights of Mnk2 kinase activation by phosphorylation to facilitate inhibitor discovery, Future Med. Chem. 7 (2015) 91—102.

[30] W. Sherman, T. Day, M.P. Jacobson, R.A. Friesner, R. Farid, Novel procedure for modeling ligand/receptor induced fit effects, J. Med. Chem. 49 (2006) 534—553.

[31] W. Sherman, H.S. Beard, R. Farid, Use of an induced fit receptor structure in virtual screening, Chem. Biol. Drug Des. 67 (2006) 83—84.

[32] S. Wang, G. Griffiths, C.A. Midgley, A.L. Barnett, M. Cooper, J. Grabarek, L. Ingram, W. Jackson, G. Kontopidis, S.J. McClue, C. McInnes, J. McLachlan, C. Meades, M. Mezna, I. Stuart, M.P. Thomas, D.I. Zheleva, D.P. Lane, R.C. Jackson, D.M. Glover, D.G. Blake, P.M. Fischer, Discovery and characterization of 2-anilino-4-(thiazol-5-yl)pyrimidine transcriptional CDK inhibitors as anticancer agents, Chem. Biol. 17 (2010) 1111—1121.

[33] S. Wang, C. Meades, G. Wood, A. Osnowski, S. Anderson, R. Yuill, M. Thomas, M. Mezna, W. Jackson, C. Midgley, G. Griffiths, I. Fleming, S. Green, I. McNae, S.-Y. Wu, C. McInnes, D. Zheleva, M.D. Walkinshaw, P.M. Fischer, 2-Anilino-4-(thiazol-5-yl)pyrimidine CDK inhibitors: synthesis, SAR analysis, X-ray crystallography, and biological activity, J. Med. Chem. 47 (2004) 1662—1675.